

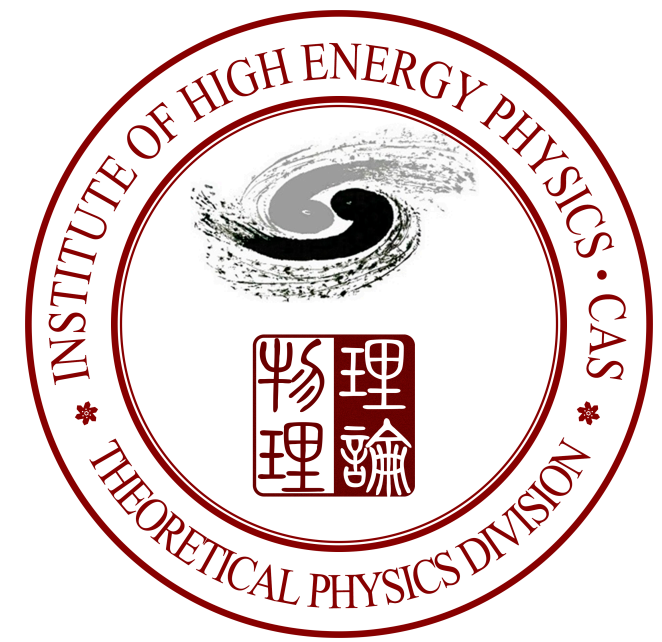
Top FCNC at future lepton colliders

Cen Zhang

Institute of High Energy Physics

EF04 Topical Group Community Meeting
CERN Dec 4 2020

Based on 1906.04573 with Liaoshan Shi
and Snowmass LOI with Gauthier Durieux, Stefano Frixione, Benjamin Fuks,
Hua-Sheng Shao, Liaoshan Shi, Marco Zaro, Xiaoran Zhao

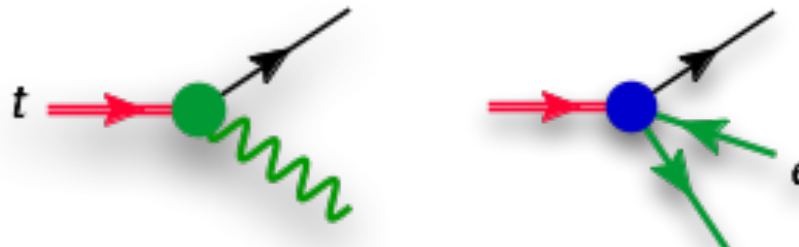


Outline

- Single top at CEPC via top FCNC
- Plan for Snowmass LOI

Top FCNC

- Neutral couplings that involve one top quark and one light quark.



- Forbidden in the SM (by GIM mechanism)
Definite sign of BSM.

	Br^{SM}	Br^{exp}
$t \rightarrow cg$	$\sim 10^{-11}$	$\lesssim 10^{-4*}$
$t \rightarrow c\gamma$	$\sim 10^{-12}$	$\lesssim 10^{-3*}$
$t \rightarrow cZ$	$\sim 10^{-13}$	$\lesssim 10^{-4}$
$t \rightarrow ch$	$\sim 10^{-14}$	$\lesssim 10^{-3}$

- A complete and systematic description of FCNC interactions based on **Standard Model Effective Field Theory**:

$$\mathcal{L}_{\text{EFT}} = \mathcal{L}_{\text{SM}} + \sum_i \frac{f_i^{(6)} O_i^{(6)}}{\Lambda^2} + \sum_i \frac{f_i^{(8)} O_i^{(8)}}{\Lambda^4} + \dots$$

Leading dim-6 FCNC operators are classified in the TOP WG EFT notes.

[Aguilar-Saavedra et al. '18]

Top FCNC

[Aguilar-Saavedra et al. '18]

[G. Durieux, the CLIC Potential for New Physics, Sec. 3.1.2, '18]

Warsaw basis operators

[B. Grzadkowski et al. 10]

$$\begin{aligned}
 O_{u\varphi}^{(ij)} &= \bar{q}_i u_j \tilde{H} (H^\dagger H), & O_{lq}^{1(ijkl)} &= (\bar{l}_i \gamma^\mu l_j) (\bar{q}_k \gamma^\mu q_l), \\
 O_{\varphi q}^{1(ij)} &= (H^\dagger \not{D}_\mu H) (\bar{q}_i \gamma^\mu q_j), & O_{lq}^{3(ijkl)} &= (\bar{l}_i \gamma^\mu \tau^I l_j) (\bar{q}_k \gamma^\mu \tau^I q_l), \\
 O_{\varphi q}^{3(ij)} &= (H^\dagger \not{D}_\mu^I H) (\bar{q}_i \gamma^\mu \tau^I q_j), & O_{lu}^{(ijkl)} &= (\bar{l}_i \gamma^\mu l_j) (\bar{u}_k \gamma^\mu u_l), \\
 O_{\varphi u}^{(ij)} &= (H^\dagger \not{D}_\mu H) (\bar{u}_i \gamma^\mu u_j), & O_{eq}^{(ijkl)} &= (\bar{e}_i \gamma^\mu e_j) (\bar{q}_k \gamma^\mu q_l), \\
 O_{\varphi ud}^{(ij)} &= (\tilde{H}^\dagger i D_\mu H) (\bar{u}_i \gamma^\mu d_j), & O_{eu}^{(ijkl)} &= (\bar{e}_i \gamma^\mu e_j) (\bar{u}_k \gamma^\mu u_l), \\
 O_{uW}^{(ij)} &= (\bar{q}_i \sigma^{\mu\nu} \tau^I u_j) \tilde{H} W_{\mu\nu}^I, & O_{lequ}^{1(ijkl)} &= (\bar{l}_i e_j) \varepsilon (\bar{q}_k u_l), \\
 O_{dW}^{(ij)} &= (\bar{q}_i \sigma^{\mu\nu} \tau^I d_j) H W_{\mu\nu}^I, & O_{lequ}^{3(ijkl)} &= (\bar{l}_i \sigma^{\mu\nu} e_j) \varepsilon (\bar{q}_k \sigma_{\mu\nu} u_l), \\
 O_{uB}^{(ij)} &= (\bar{q}_i \sigma^{\mu\nu} u_j) \tilde{H} B_{\mu\nu}, & O_{ledq}^{(ijkl)} &= (\bar{l}_i e_j) (\bar{d}_k q_l) (\bar{u}_k \gamma^\mu u_l), \\
 O_{uG}^{(ij)} &= (\bar{q}_i \sigma^{\mu\nu} T^A u_j) \tilde{H} G_{\mu\nu}^A.
 \end{aligned}$$

Relevant D.o.F for tops

[Aguilar-Saavedra et al. '18]

$$\begin{aligned}
 c_{lq}^{-[I](1,3+a)} &\equiv \Re\{C_{lq}^{-(113a)}\}, & c_{eq}^{[I](1,3+a)} &\equiv \Re\{C_{eq}^{(113a)}\}, \\
 c_{\varphi q}^{-[I](3+a)} &\equiv \Re\{C_{\varphi q}^{1(3a)} - C_{\varphi q}^{3(3a)}\}, & c_{lu}^{[I](1,3+a)} &\equiv \Re\{C_{lu}^{(113a)}\}, \\
 c_{\varphi u}^{[I](3+a)} &\equiv \Re\{C_{\varphi u}^{(3a)}\}, & c_{eu}^{[I](1,3+a)} &\equiv \Re\{C_{eu}^{(113a)}\}, \\
 c_{uA}^{[I](3a)} &\equiv \Re\{c_W C_{uB}^{(3a)} + s_W C_{uW}^{(3a)}\}, & c_{lequ}^{S[I](1,3a)} &\equiv \Re\{C_{lequ}^{1(113a)}\}, \\
 c_{uA}^{[I](a3)} &\equiv \Re\{c_W C_{uB}^{(a3)} + s_W C_{uW}^{(a3)}\}, & c_{lequ}^{S[I](1,a3)} &\equiv \Re\{C_{lequ}^{1(11a3)}\}, \\
 c_{uZ}^{[I](3a)} &\equiv \Re\{-s_W C_{uB}^{(3a)} + c_W C_{uW}^{(3a)}\}, & c_{lequ}^{T[I](1,3a)} &\equiv \Re\{C_{lequ}^{3(113a)}\}, \\
 c_{uZ}^{[I](a3)} &\equiv \Re\{-s_W C_{uB}^{(a3)} + c_W C_{uW}^{(a3)}\}, & c_{lequ}^{T[I](1,a3)} &\equiv \Re\{C_{lequ}^{3(11a3)}\}.
 \end{aligned}$$

No interference between rows, sufficient to focus on 7 parameters at a time

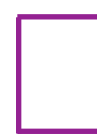
28 DoFs relevant for ee->tj

$$\begin{aligned}
 &c_{lq}^{-(1,3+a)}, c_{eq}^{(1,3+a)}, c_{\varphi q}^{-(3+a)}, c_{uA}^{(a3)}, c_{uZ}^{(a3)}, c_{lequ}^{S(1,a3)}, c_{lequ}^{T(1,a3)}, \\
 &c_{lu}^{(1,3+a)}, c_{eu}^{(1,3+a)}, c_{\varphi u}^{(3+a)}, c_{uA}^{(3a)}, c_{uZ}^{(3a)}, c_{lequ}^{S(1,3a)}, c_{lequ}^{T(1,3a)}, \\
 &c_{lq}^{-I(1,3+a)}, c_{eq}^{I(1,3+a)}, c_{\varphi q}^{-I(3+a)}, c_{uA}^{I(a3)}, c_{uZ}^{I(a3)}, c_{lequ}^{SI(1,a3)}, c_{lequ}^{TI(1,a3)}, \\
 &c_{lu}^{I(1,3+a)}, c_{eu}^{I(1,3+a)}, c_{\varphi u}^{I(3+a)}, c_{uA}^{I(3a)}, c_{uZ}^{I(3a)}, c_{lequ}^{SI(1,3a)}, c_{lequ}^{TI(1,3a)},
 \end{aligned}$$

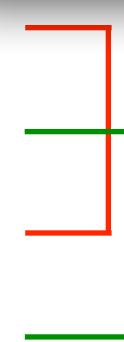
CP even



CP odd



Left-handed q



Right-handed q

a=1: tuV/tull

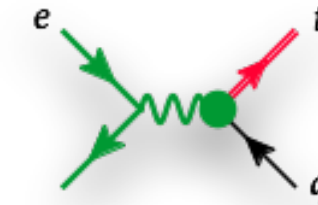
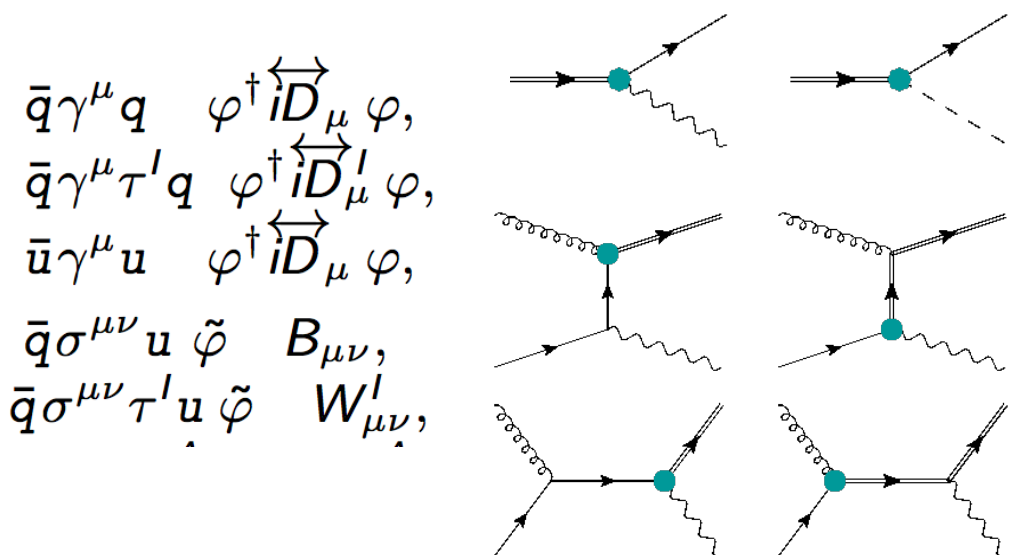
a=2: tcV/tcll

Top FCNC: 2-fermion operators

28 DoFs relevant for ee

$$\begin{array}{lll}
 c_{\varphi q}^{-(3+a)}, & c_{uA}^{(a3)}, & c_{uZ}^{(a3)}, \\
 c_{\varphi u}^{(3+a)}, & c_{uA}^{(3a)}, & c_{uZ}^{(3a)}, \\
 c_{\varphi q}^{-I(3+a)}, & c_{uA}^{I(a3)}, & c_{uZ}^{I(a3)}, \\
 c_{\varphi u}^{I(3+a)}, & c_{uA}^{I(3a)}, & c_{uZ}^{I(3a)}, \\
 c_{lequ}^{S(1,a3)}, & c_{lequ}^{T(1,a3)}, & c_{lq}^{-(1,3+a)}, \\
 c_{lequ}^{S(1,3a)}, & c_{lequ}^{T(1,3a)}, & c_{lu}^{(1,3+a)}, \\
 c_{lequ}^{SI(1,a3)}, & c_{lequ}^{TI(1,a3)}, & c_{lq}^{-I(1,3+a)}, \\
 c_{lequ}^{SI(1,3a)}, & c_{lequ}^{TI(1,3a)}, & c_{lu}^{I(1,3+a)}, \\
 & & c_{eq}^{I(1,3+a)}
 \end{array}$$

2-fermion FCNC



FCC-ee: [H. Khanpour et al. 1408.2090]

Integrated luminosity	Branching ratio	240 GeV	350 GeV	500 GeV
300 fb ⁻¹	$Br(t \rightarrow q\gamma)$	1.23×10^{-4}	3.43×10^{-5}	2.45×10^{-5}
	$Br(t \rightarrow qZ) (\sigma_{\mu\nu})$	1.50×10^{-4}	4.97×10^{-5}	3.94×10^{-5}
	$Br(t \rightarrow qZ) (\gamma_\mu)$	3.06×10^{-4}	1.83×10^{-4}	2.67×10^{-4}
3 ab ⁻¹	$Br(t \rightarrow q\gamma)$	3.70×10^{-5}	9.86×10^{-6}	6.76×10^{-6}
	$Br(t \rightarrow qZ) (\sigma_{\mu\nu})$	4.50×10^{-5}	1.41×10^{-5}	1.09×10^{-5}
	$Br(t \rightarrow qZ) (\gamma_\mu)$	9.25×10^{-5}	5.27×10^{-5}	7.49×10^{-4}
10 ab ⁻¹	$Br(t \rightarrow q\gamma)$	2.01×10^{-5}	5.25×10^{-6}	3.59×10^{-6}
	$Br(t \rightarrow qZ) (\sigma_{\mu\nu})$	2.44×10^{-5}	7.60×10^{-6}	5.85×10^{-6}
	$Br(t \rightarrow qZ) (\gamma_\mu)$	5.02×10^{-5}	2.83×10^{-5}	4.00×10^{-5}

ILC 500: [Aguilar–Saavedra & Riemann '01]

CLIC: [G. Durieux, the CLIC Potential for New Physics, Sec.3.1.2, 18]

Goal 1: have similar results for CEPC

Top FCNC: 4-fermion operators

28 DoFs relevant for ee

$c_{\varphi q}^{-(3+a)}, c_{uA}^{(a3)}, c_{uZ}^{(a3)}, c_{lequ}^{S(1,a3)}, c_{lequ}^{T(1,a3)}, c_{lq}^{-(1,3+a)}, c_{eq}^{(1,3+a)}$	$c_{\varphi u}^{(3+a)}, c_{uA}^{(3a)}, c_{uZ}^{(3a)}, c_{lequ}^{S(1,3a)}, c_{lequ}^{T(1,3a)}, c_{lu}^{(1,3+a)}, c_{eu}^{(1,3+a)}$
$c_{\varphi q}^{-I(3+a)}, c_{uA}^{I(a3)}, c_{uZ}^{I(a3)}, c_{lequ}^{SI(1,a3)}, c_{lequ}^{TI(1,a3)}, c_{lq}^{-I(1,3+a)}, c_{eq}^{I(1,3+a)}$	$c_{\varphi u}^{I(3+a)}, c_{uA}^{I(3a)}, c_{uZ}^{I(3a)}, c_{lequ}^{SI(1,3a)}, c_{lequ}^{TI(1,3a)}, c_{lu}^{I(1,3+a)}, c_{eu}^{I(1,3+a)}$

↓

4-fermion FCNC

UV

EFT

$\mathcal{L}_{tceee} = \frac{1}{\Lambda^2} \sum_{i,j=L,R} \left[V_{ij} (\bar{e} \gamma_\mu P_i e) (\bar{t} \gamma^\mu P_j c) + S_{ij} (\bar{e} P_i e) (\bar{t} P_j c) + T_{ij} (\bar{e} \sigma_{\mu\nu} P_i e) (\bar{t} \sigma_{\mu\nu} P_j c) \right],$

[Bar-Shalom, Wudka '99]

Best bounds still from LEP2!

Scenario	Hadronic topology				Semi-leptonic topology				Combined topologies			
	obs.	-1 σ	exp.	+1 σ	obs.	-1 σ	exp.	+1 σ	obs.	-1 σ	exp.	+1 σ
SVT	1218	1268	1180	1097	1315	1406	1301	1203	1402	1468	1366	1264
S	577	604	556	520	647	647	603	555	685	693	641	593
V	953	1003	933	863	997	1069	997	921	1073	1141	1068	980
T	1069	1117	1045	969	1124	1232	1142	1052	1204	1300	1210	1114

Table 5: Observed and expected 95% CL lower limits on Λ (GeV)
[DELPHI, CERN-PH-EP/2010-056]

CLIC: [G. Durieux, the CLIC Potential for New Physics, Sec.3.1.2, '18]

Currently no results for FCC-ee and ILC

No dedicated search ($t>qZ$) at the LHC
(Recast from $t>qZ$ is possible
[Chala, Santiago, Spannowsky '18])

Goal 2: study 4-f operators at CEPC

Top FCNC: current/future limits

[HL/HE YR, 1812.07638]

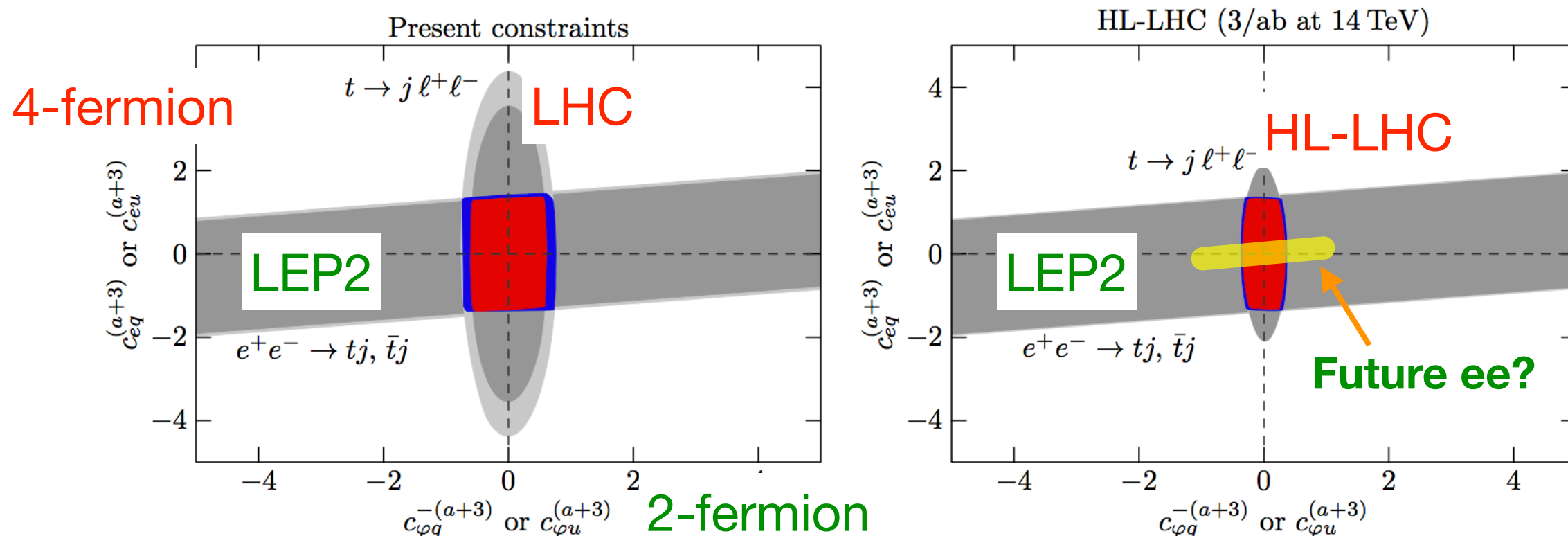
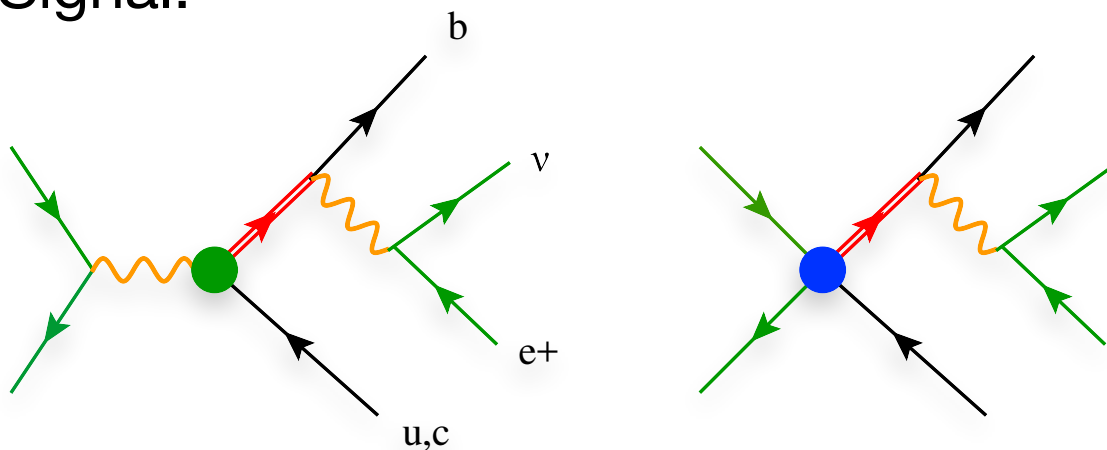


Fig. 59: Current (left) and prospective HL-LHC (right) 95% C.L. limits on top-quark FCNC operator coefficients in a two-dimensional plane formed by two- (x axis) and four-fermion (y axis) operator coefficients. Other parameters are marginalized over, within the constraints obtained when all measurements are included. Red and blue regions are the combined constraints for top-up and top-charm FCNCs. The impact of $t \rightarrow j \ell^+ \ell^-$ and $e^+ e^- \rightarrow tj, \bar{t}j$ measurements is displayed separately in dark and light gray colors for top-up and top-charm FCNCs, respectively.

Goal 3: confirm the same complementarity between HL-LHC and CEPC

The analysis

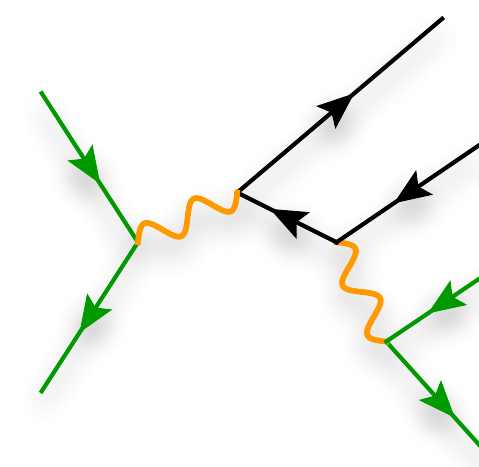
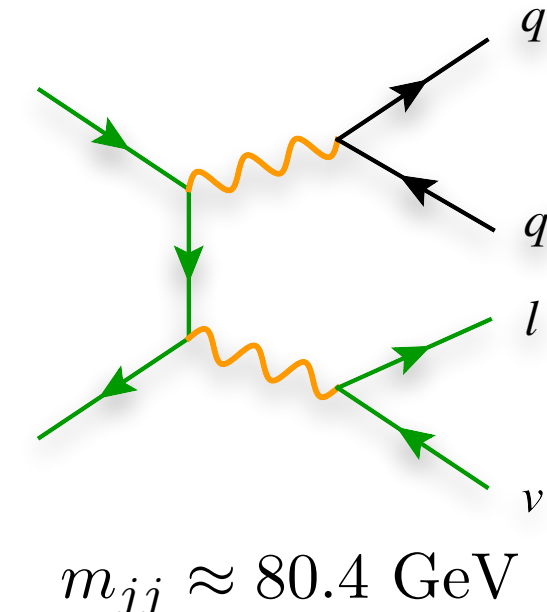
- CEPC scenario, 240 GeV, 5.6 ab^{-1}
 - Expect similar results for FCC-ee 240 GeV 5 ab^{-1} .
- LO+PS, with MadGraph5 and Pythia8
- FCNC implementation: **dim6top**
<https://feynrules.irmp.ucl.ac.be/wiki/dim6top>
- Detector effects: Delphes with CEPC card
- Signal:



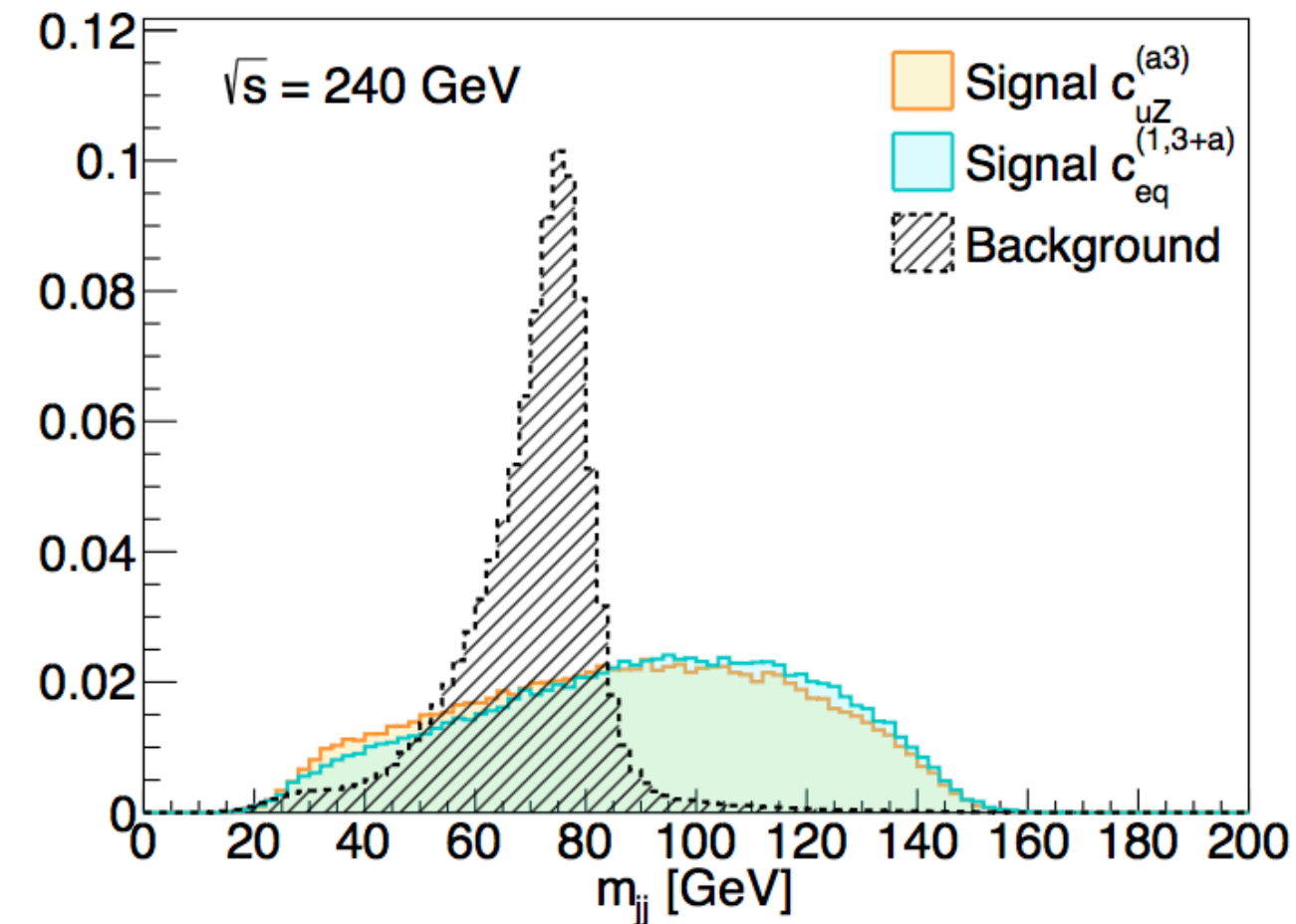
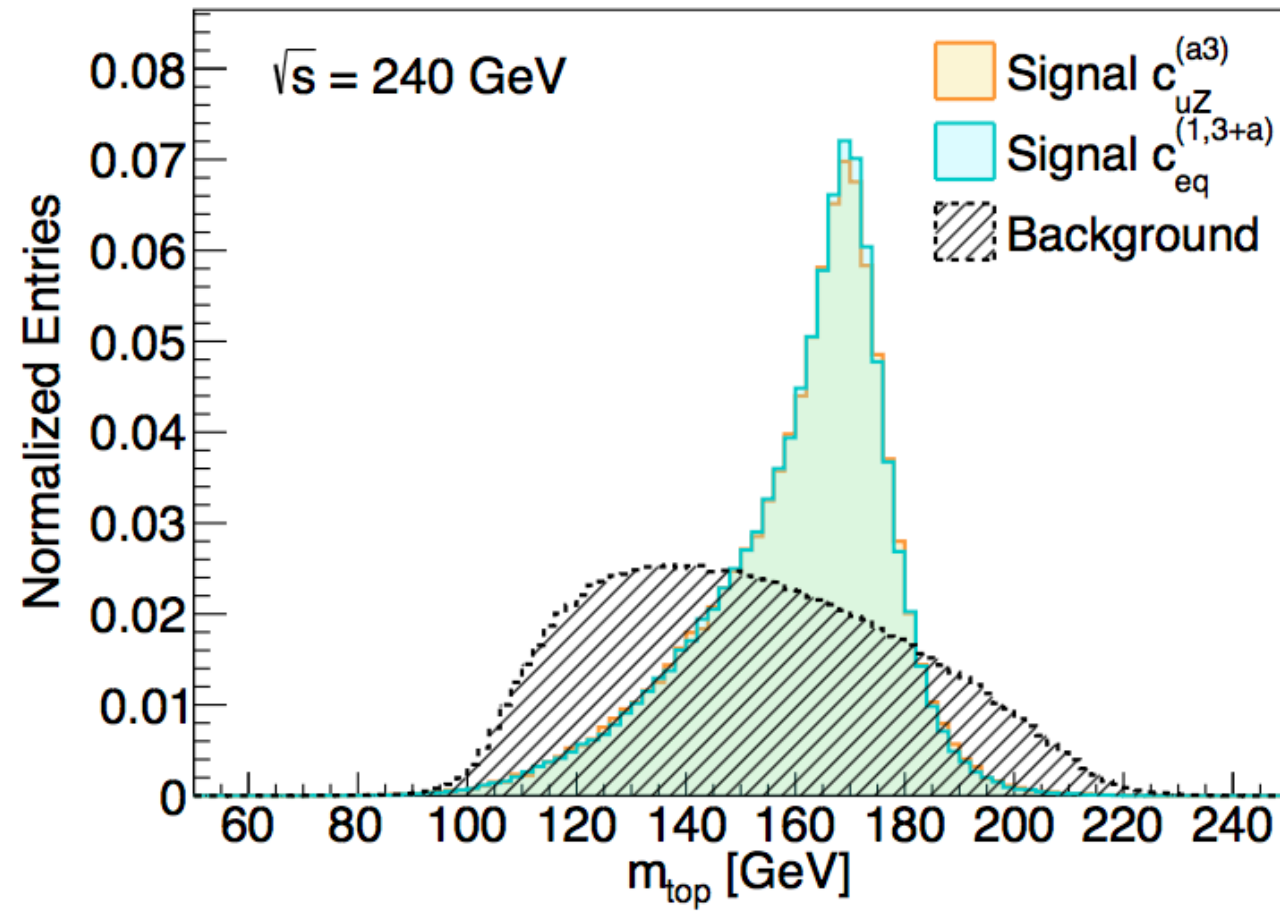
$$m_{top,rec} \approx 172.5 \text{ GeV}$$

$$E_{j,rec} \approx \frac{s - m_t^2}{2\sqrt{s}} \approx 58 \text{ GeV}$$

- Background: Wjj dominant



- $+ Zjj$



Baseline scenario: use simple cuts

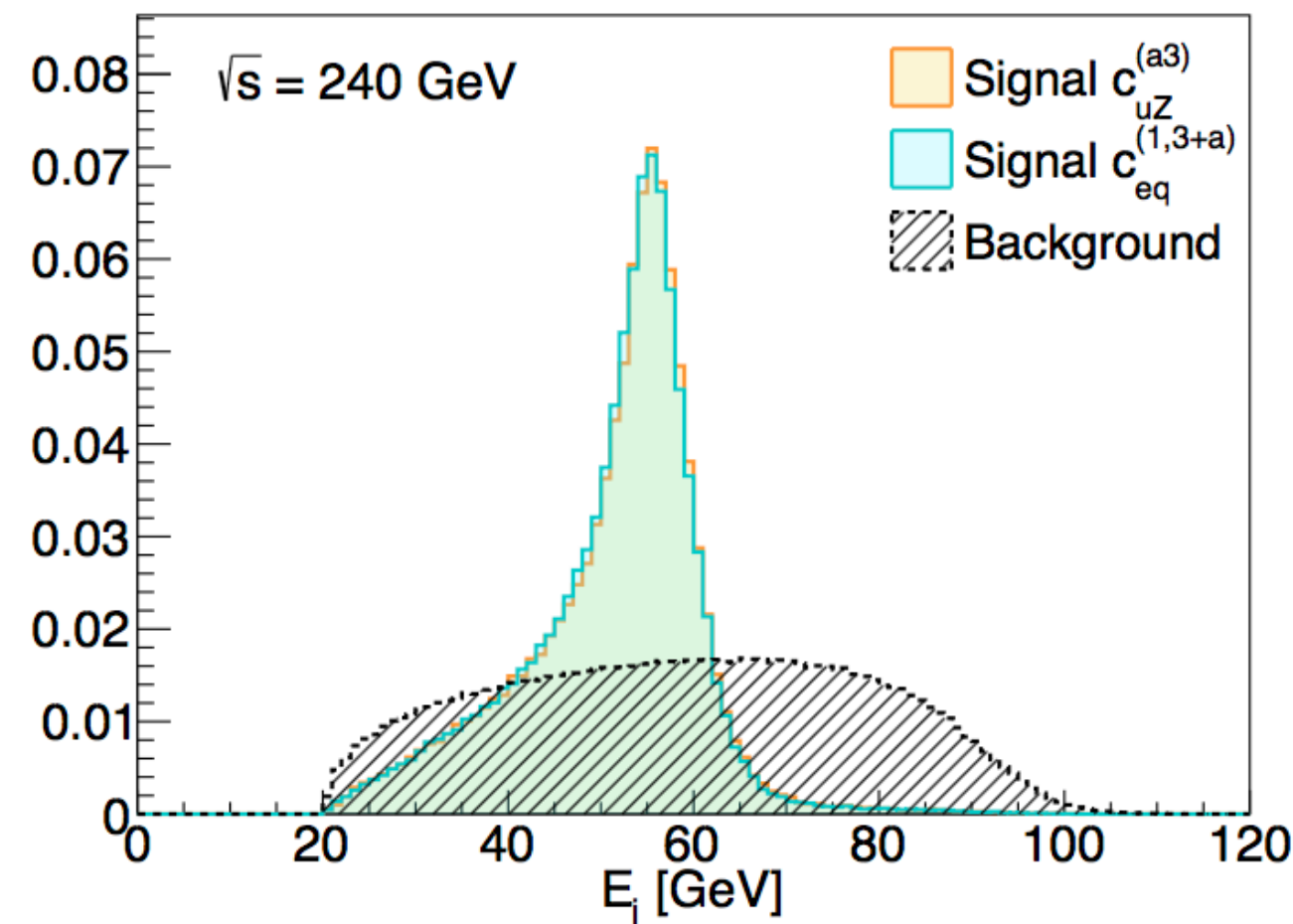
$E_j < 60 \text{ GeV}$, exactly 1 b -tagged jet

$m_{jj} > 100 \text{ GeV}$,

$m_{top} < 180 \text{ GeV}$.

1400 events at 5.6 ab^{-1}
 $\rightarrow 95\% \text{ CL limit on xsec: } 0.0134 \text{ fb}$

Needs to be translated to operators coeffs...



EFT parameter space

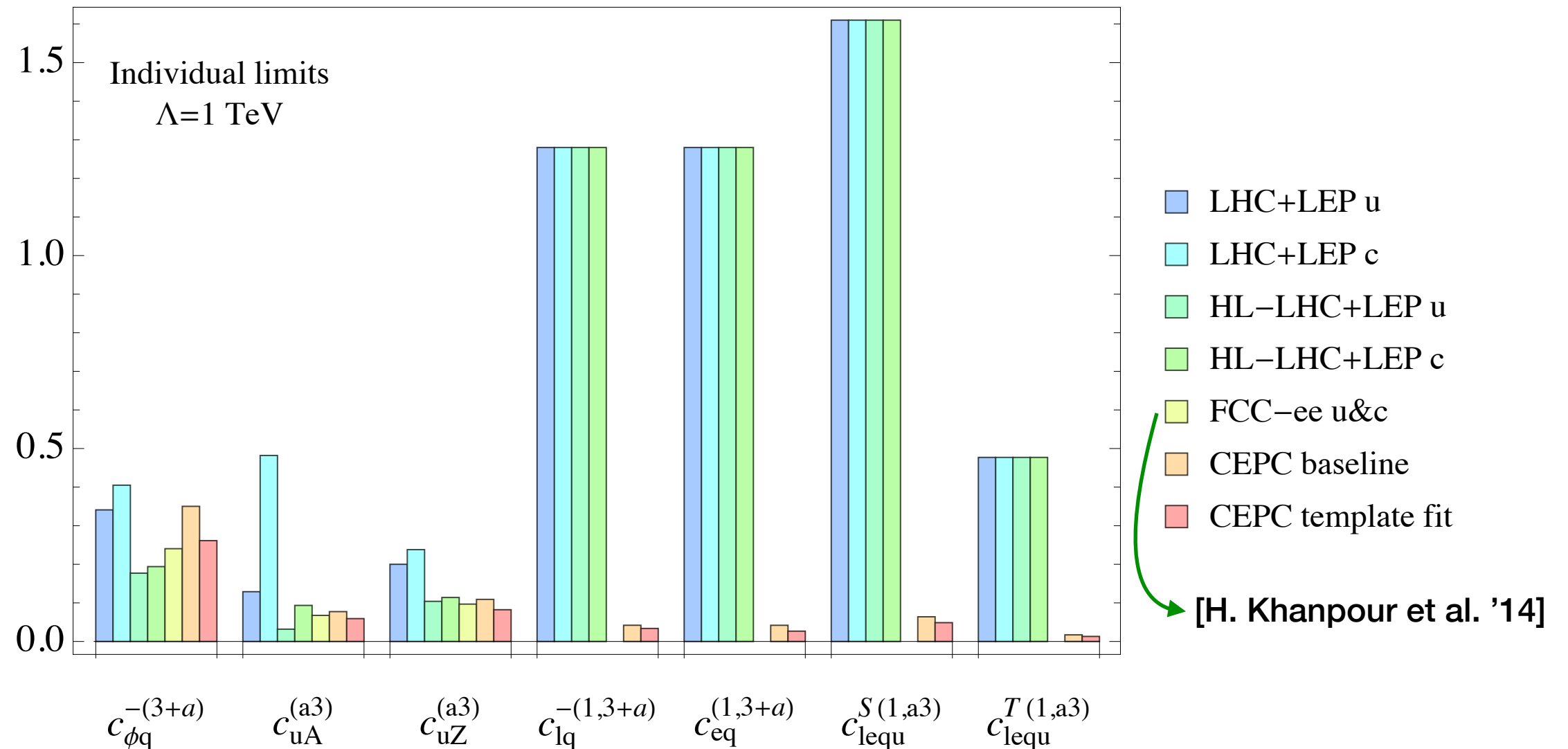
28 DoFs relevant for ee->tj

$$\begin{aligned}
 & c_{lq}^{-(1,3+a)}, \quad c_{eq}^{(1,3+a)}, \quad c_{\varphi q}^{-(3+a)}, \quad c_{uA}^{(a3)}, \quad c_{uZ}^{(a3)}, \quad c_{lequ}^{S(1,a3)}, \quad c_{lequ}^{T(1,a3)}, \\
 & c_{lu}^{(1,3+a)}, \quad c_{eu}^{(1,3+a)}, \quad c_{\varphi u}^{(3+a)}, \quad c_{uA}^{(3a)}, \quad c_{uZ}^{(3a)}, \quad c_{lequ}^{S(1,3a)}, \quad c_{lequ}^{T(1,3a)}, \\
 & c_{lq}^{-I(1,3+a)}, \quad c_{eq}^{I(1,3+a)}, \quad c_{\varphi q}^{-I(3+a)}, \quad c_{uA}^{I(a3)}, \quad c_{uZ}^{I(a3)}, \quad c_{lequ}^{SI(1,a3)}, \quad c_{lequ}^{TI(1,a3)}, \\
 & c_{lu}^{I(1,3+a)}, \quad c_{eu}^{I(1,3+a)}, \quad c_{\varphi u}^{I(3+a)}, \quad c_{uA}^{I(3a)}, \quad c_{uZ}^{I(3a)}, \quad c_{lequ}^{SI(1,3a)}, \quad c_{lequ}^{TI(1,3a)},
 \end{aligned}$$

$$\sigma_{\text{signal}} = \sum_{1 \leq i \leq j \leq 7} \frac{C_i C_j}{\Lambda^4} \sigma_{ij}$$

- σ_{ij} : $7 \times 8 \div 2 = 28$ independent terms.
- They are determined by simulating the signal at 28 sampling points in the 7-D parameter space and fitting to a polynomial.
- With these, the limit on xsec is converted to 95% 7-D bound in the dim-6 parameter space.

Bounds on individual operators



FCC-ee: 4f operator limits are not available; 2f slightly better

[H. Khanpour et al. '14]

CLIC: 380 GeV run + polarization, 3~4 times better on 4f

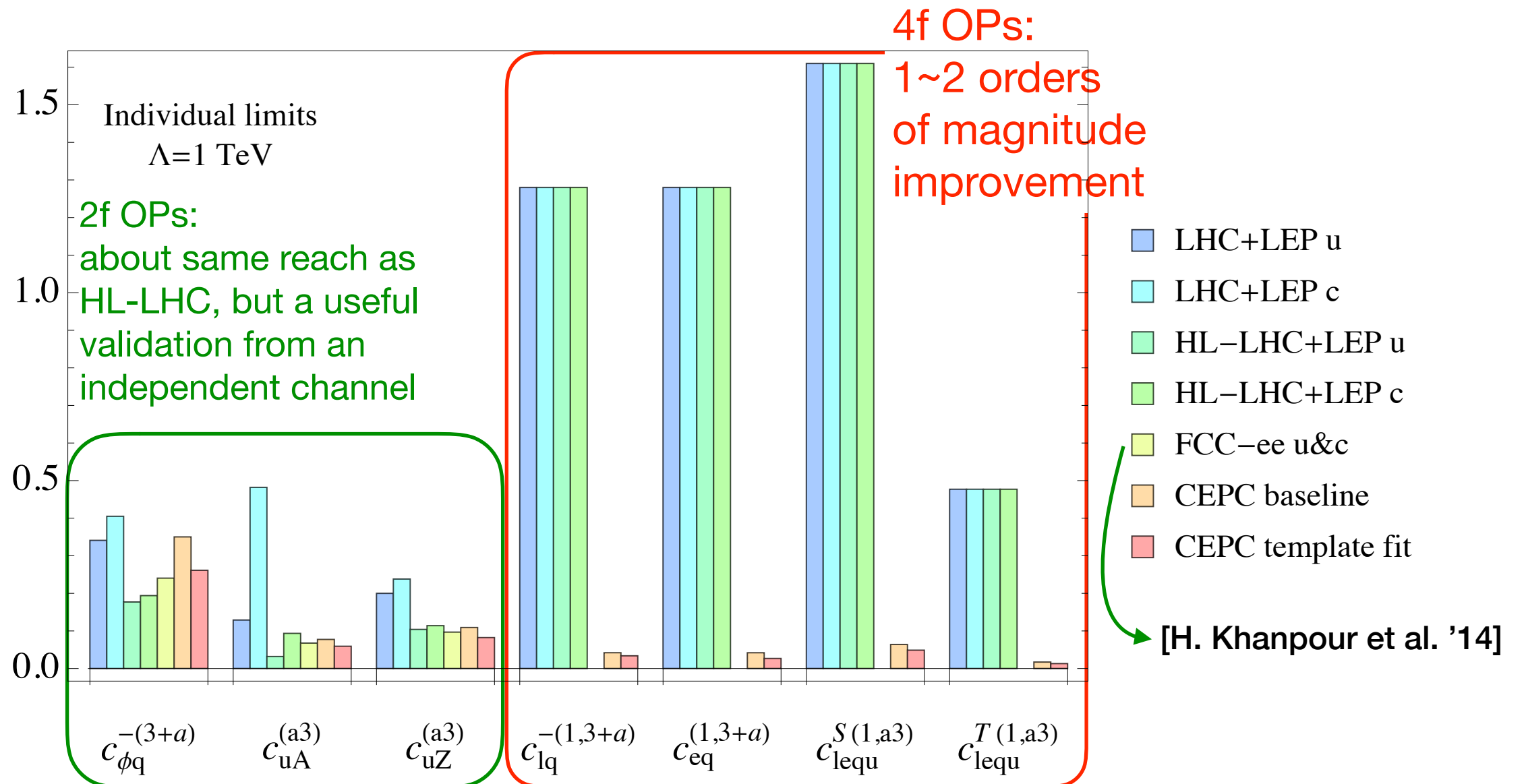
Larger energy \rightarrow better limits

[G. Durieux, the CLIC Potential for New Physics, CERN YR, 18]

LHeC: similar limits

[W. Liu, H. Sun 1906.04884]

Bounds on individual operators



FCC-ee: 4f operator limits are not available; 2f slightly better

[H. Khanpour et al. '14]

CLIC: 380 GeV run + polarization, 3~4 times better on 4f

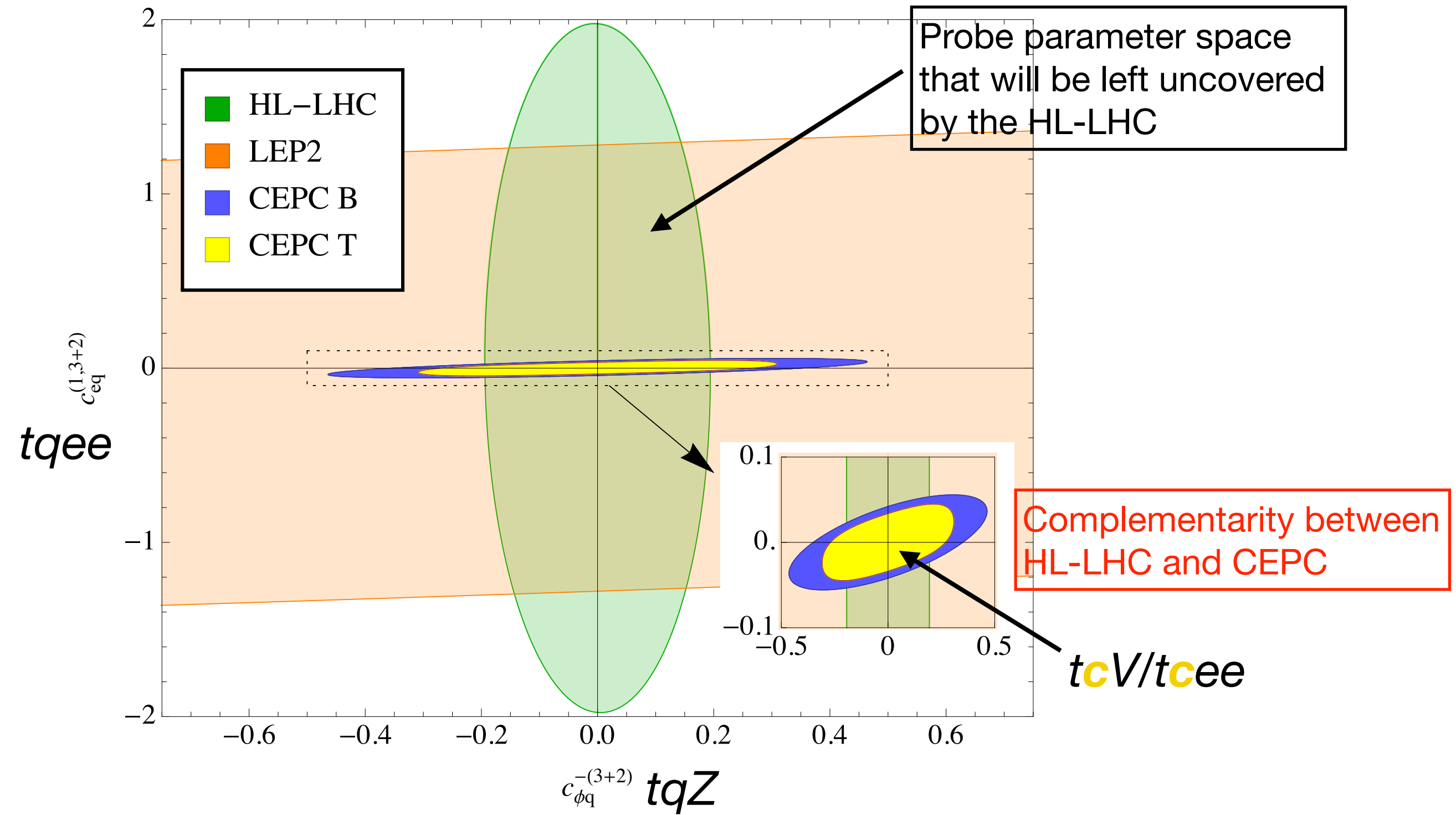
Larger energy \rightarrow better limits

[G. Durieux, the CLIC Potential for New Physics, CERN YR, 18]

LHeC: similar limits

[W. Liu, H. Sun 1906.04884]

Bounds on 2f vs 4f operators: HL-LHC + CEPC



Improving with a “template fit”

- To further improve, we also consider:

- Angular distribution:

Signal produced by different operators with different Lorentz structures can be distinguished by production angle

→ **This will improve the discrimination power** between different operators

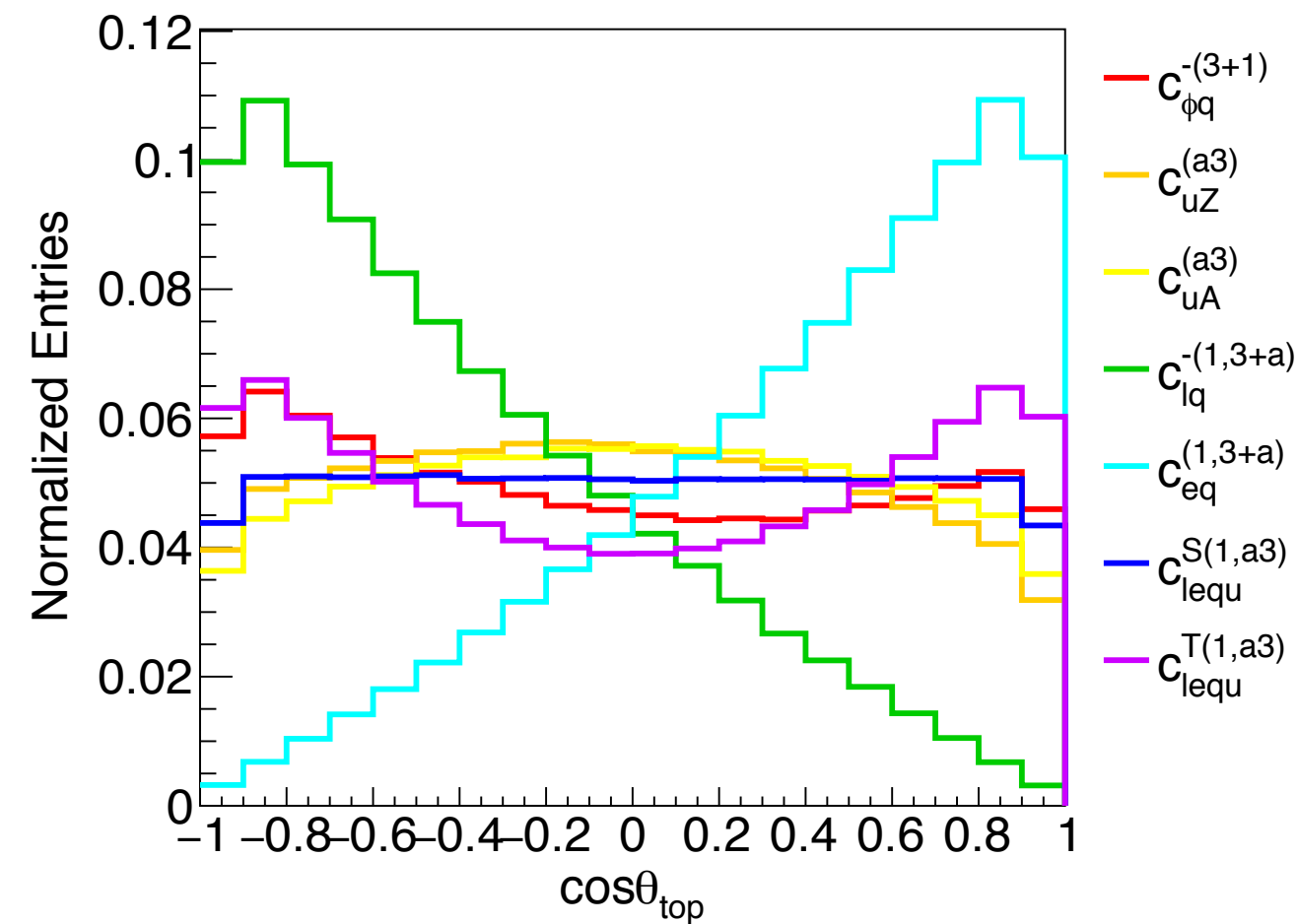
- Charm tagging: (has been mentioned in [H. Khanpour et al. 1408.2090])

For tcV/tcee operators, the signal is b, c, l, ν while the main background is c, s, l, ν where the c fakes the b. So choosing a c-tagged jet improves S/B.

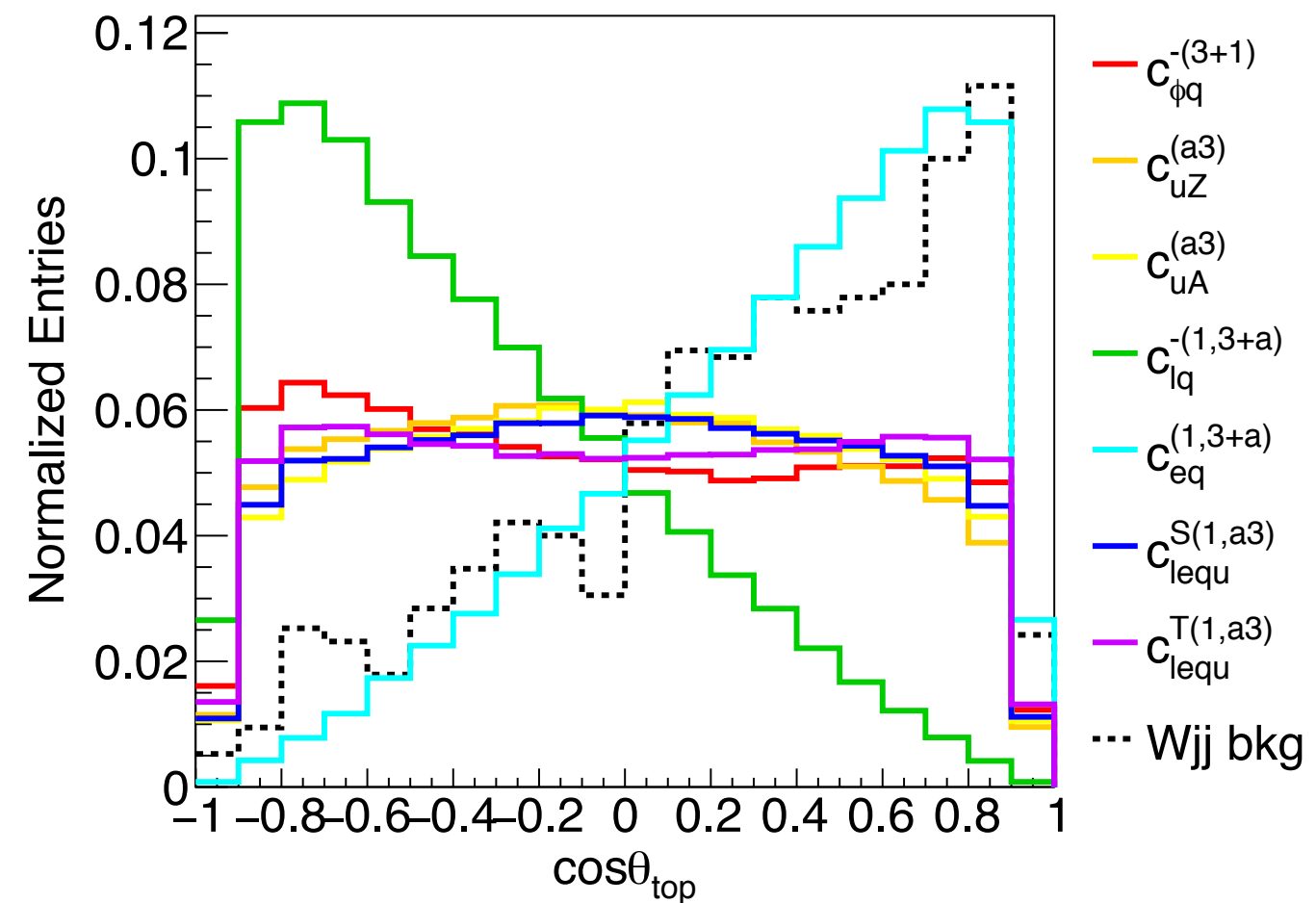
→ **This will improve sensitivity on a=2 operators.** (i.e. tcV/tcee)

Angular distribution

Parton level



Reconstructed



Template fit: divide the signal region into 8 bins,
i.e. 4 bins in $Q_l \times \cos\theta_{top}$ + charm tagging

Improvement from c-jet tagging

If no signal is observed:

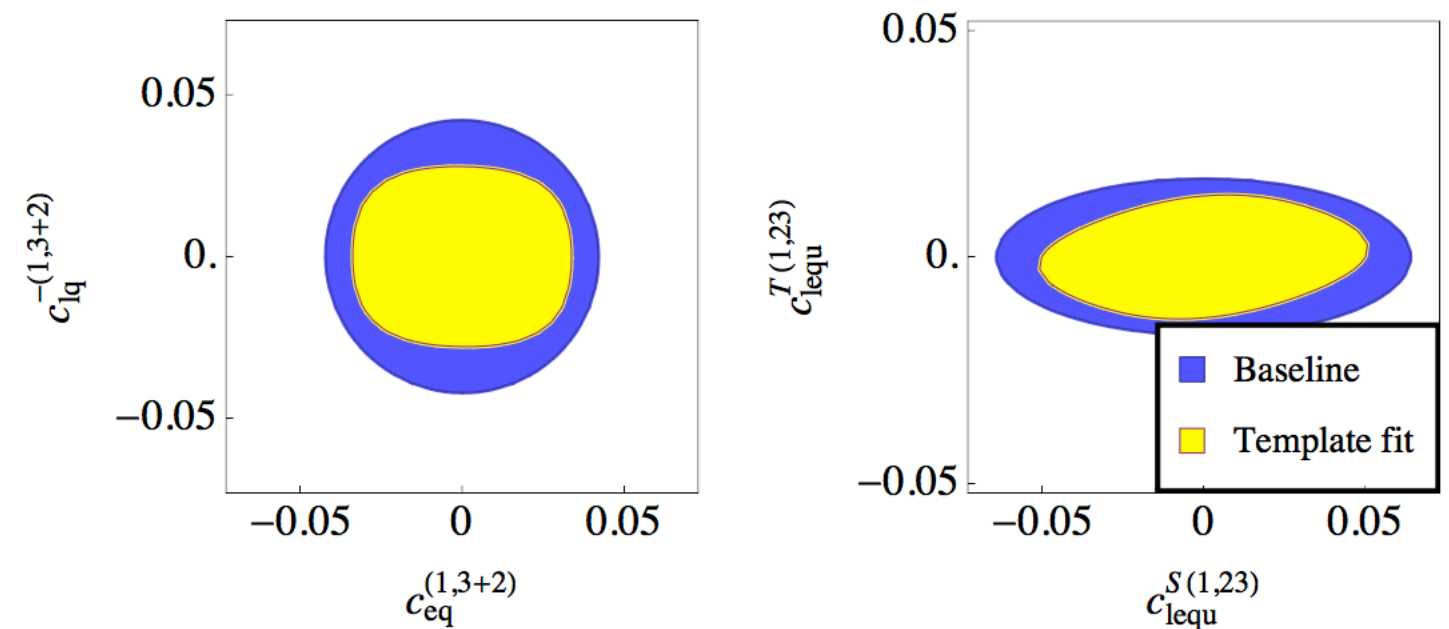
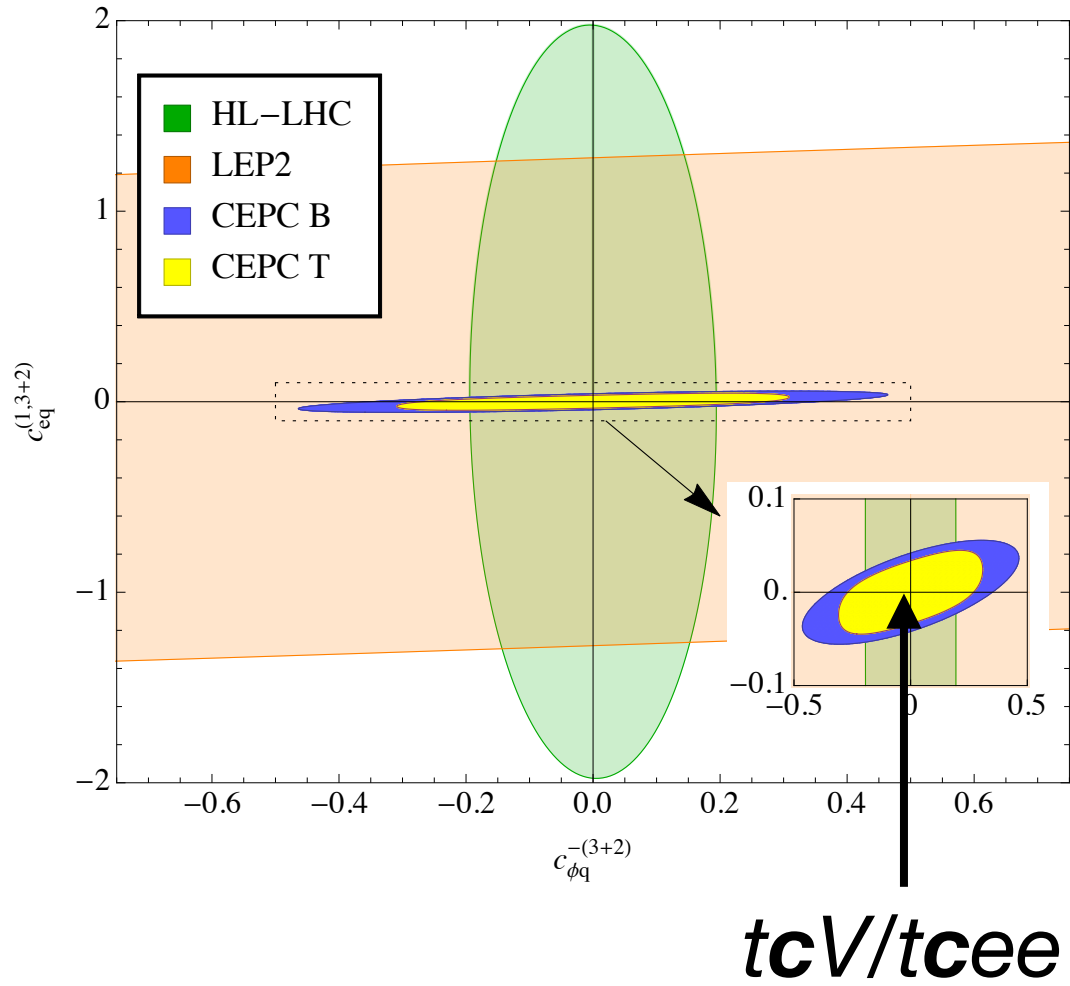


Fig. 8. Two-dimensional limits on four-fermion coefficients, at 95% CL, under the SM hypothesis, with other coefficients turned off. The template fit approach improves the sensitivity.

Discriminating between different operators, when an excess is observed

Using angular observable

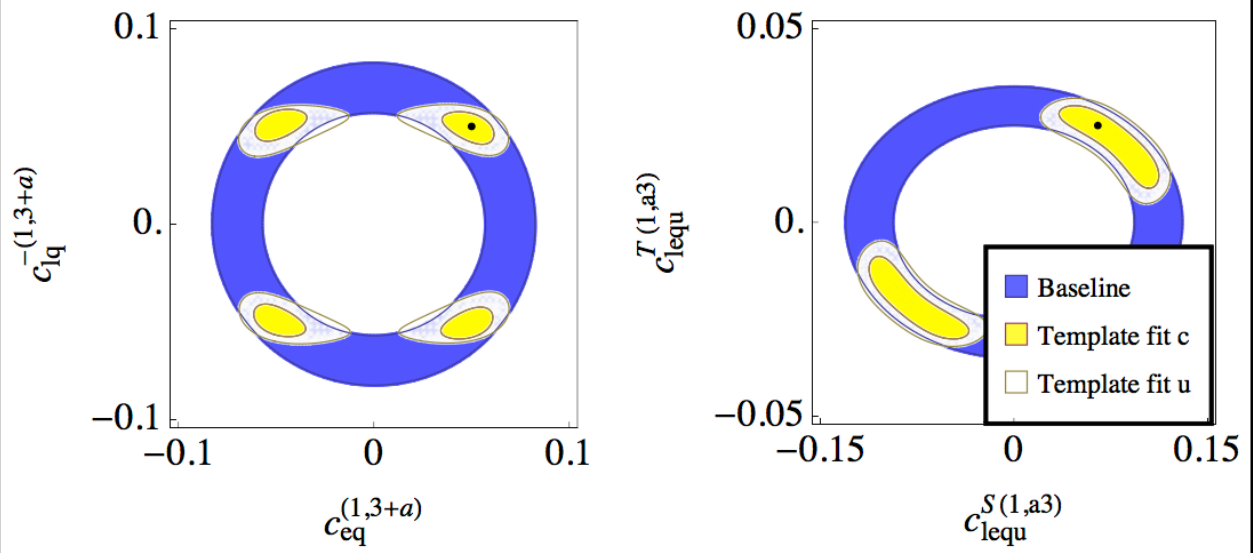


Fig. 9. Two-dimensional limits on four-fermion coefficients, at 95% CL, with other coefficients turned off. Two hypotheses are considered. Left: $c_{eq}^{(1,3+a)} = c_{lq}^{-(1,3+a)} = 0.05$. Right: $c_{lequ}^{S(1,a3)} = 0.065$, $c_{lequ}^{T(1,a3)} = 0.025$. Both points are labeled by a black dot in the plots. The template fit helps to pinpoint the coefficients. Better precision is obtained for operators involving a charm-quark (i.e. $a=2$).

Using c-tagging

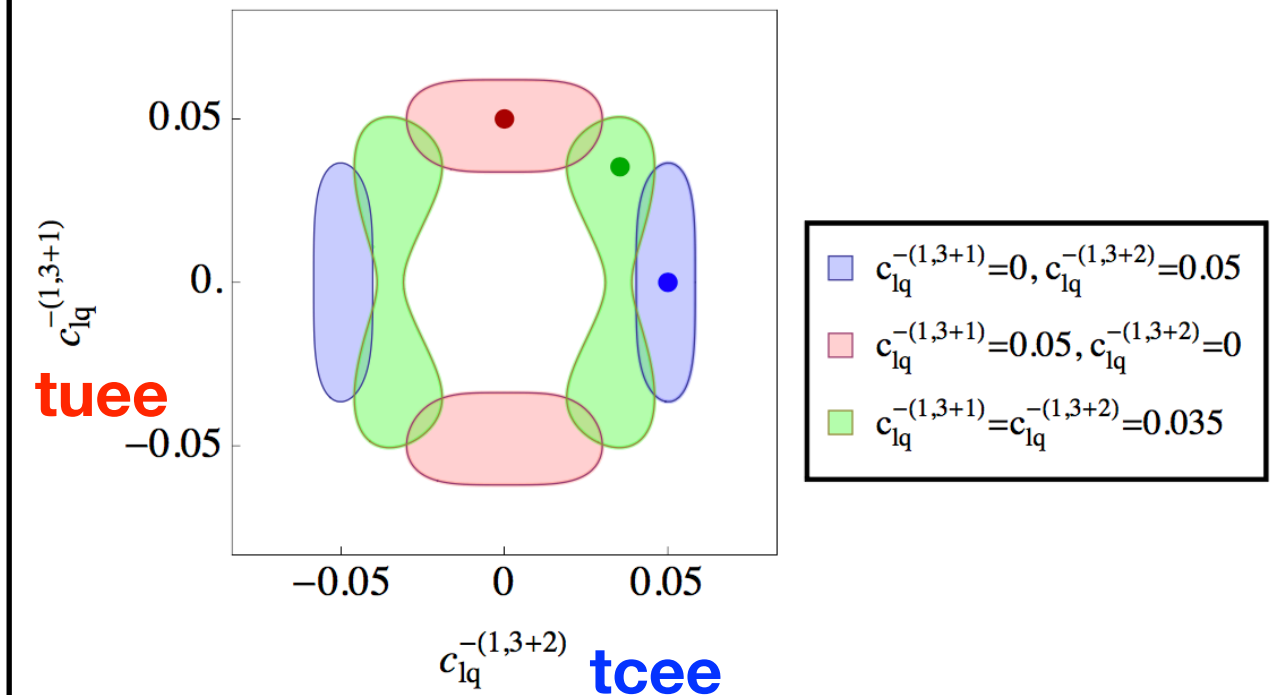


Fig. 10. Two-dimensional limits on $c_{lq}^{-(1,3+a)}$ coefficients with $a=1$ and $a=2$, at 95% CL. Other coefficients are turned off. Three hypotheses are considered. The template fit helps to identify the light-quark flavor involved in the FCN coupling.

**In contrast to LHC:
No such info from top decay**

Future plan: physics side

- Comprehensive and model-independent studies based on the SMEFT framework and including realistic collider analyses. With a focus on 4-fermion operators.
With Gauthier Durieux, Benjamin Fuks, Hua-Sheng Shao, Liaoshan Shi
- Incorporate other ee colliders, FCC-ee, ILC, CLIC
- Explore additional channels: ttbar with FCNC decay
- Improve the simulation.
 - SMEFT@NLO exists but is restricted by flavor symmetry assumptions.
 - NLO QCD for FCNC operators, consistent with LHC TOP WG. Based on [Degrande, Maltoni, Wang, CZ '14], automated with MadGraph5_aMC@NLO.
 - Four-fermion operators are now added.

Future plan: code side

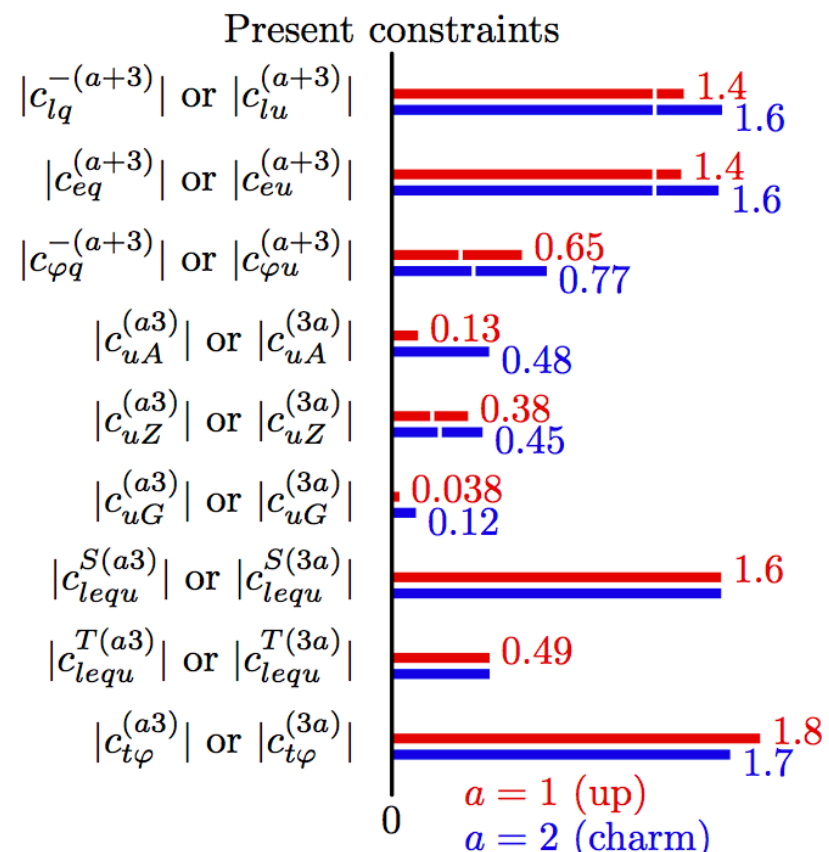
by Stefano Frixione, Marco Zaro, Xiaoran Zhao

- Test case for automatic framework that allows for general BSM to be studied at future e+e- colliders, with more reliable theory predictions, not only for the SM, but also for signals.
- ISR and beamstrahlung will be taken care of by a new MG branch. WIP.
 - Different BS scenarios will be made available and are stored as grids.
 - Difficulty is that ISR is peaked/divergent at $x > 1$.
 - LO + NLO QCD ok, also in the presence of (narrow) resonances with $m < \sim s$
 - NLL ISR by Frixione et al. will be included. NLO EW is in progress.
[1909.03886 S. Frixione], [1911.12040 Bertone, Cacciari, Frixione, Stagnitto]
- Version in development:
<https://code.launchpad.net/~maddevelopers/mg5amcnlo/2.7.3-lepcoll>
 - Set lpp1=lpp2=4 in the run_card
 - Set pdlabel to a value corresponding to one of the folders inside Source/PDF/lep_densities (cepc240ll fcce240ll fcce365ll ilc500ll isronlyll)

Thank you

Top FCNC: current limits

Mode	$\text{Br}^{95\% \text{CL}}$	Ref.	exp.	\sqrt{s}	\mathcal{L}	remarks
$t \rightarrow qZ$						
u	1.7×10^{-4}	[1176]	ATLAS	13 TeV	36.1 fb^{-1}	decay, $ m_{\ell\ell} - m_Z < 15 \text{ GeV}$
c	2.4×10^{-4}					
u	2.4×10^{-4}	[1177]	CMS	13 TeV	35.9 fb^{-1}	production plus decay
c	4.5×10^{-4}					
u	2.2×10^{-4}	[1178]	CMS	8 TeV	19.7 fb^{-1}	production, $76 < m_{\ell\ell} < 106 \text{ GeV}$
c	4.9×10^{-4}					
$t \rightarrow qg$						
u	0.40×10^{-4}	[1179]	ATLAS	8 TeV	20.3 fb^{-1}	$\sigma(pp \rightarrow t) \times \text{Br}(t \rightarrow bW) < 3.4 \text{ pb}$
c	2.0×10^{-4}					
u	0.20×10^{-4}	[1180]	CMS	7, 8 TeV	$5.0, 17.9 \text{ fb}^{-1}$	in $pp \rightarrow tj$
c	4.1×10^{-4}					
$t \rightarrow q\gamma$						
u	1.3×10^{-4}	[1175]	CMS	8 TeV	19.8 fb^{-1}	$\sigma(pp \rightarrow t\gamma) \times \text{Br}(t \rightarrow bl\nu) < 26 \text{ fb}$
c	17×10^{-4}					$\sigma(pp \rightarrow t\gamma) \times \text{Br}(t \rightarrow bl\nu) < 37 \text{ fb}$
$t \rightarrow qh$						
u	19×10^{-4}	[1181]	ATLAS	13 TeV	36.1 fb^{-1}	multilepton channel
c	16×10^{-4}					
u	55×10^{-4}	[1182]	CMS	8 TeV	19.7 fb^{-1}	multilepton, $\gamma\gamma, b\bar{b}$
c	40×10^{-4}					
u	47×10^{-4}	[1183]	CMS	13 TeV	35.9 fb^{-1}	$b\bar{b}$
c	47×10^{-4}					



[Durieux, Kitahara, CZ '18]

Top FCNC: 4-fermion operators from LHC

[Chala, Santiago, Spannowsky '18]

- Recast $t \rightarrow qZ \rightarrow ee$ at LHC is possible (though this suffers from the M_{ee} mass window cut.)
- Recast limits from LHC:

	$c_{lq}^{-(2223)}$	$c_{eq}^{(2223)}$	$c_{lu}^{(2223)}$	$c_{eu}^{(2223)}$	$c_{lequ}^{1(2223)}$	$c_{lequ}^{1(2232)}$	$c_{lequ}^{3(2223)}$	$c_{lequ}^{3(2232)}$
CR1	8.4 (1.2)	8.4 (1.2)	8.4 (1.2)	8.4 (1.2)	18 (2.7)	18 (2.7)	2.3 (0.35)	2.3 (0.35)
NEW	3.1 (1.0)	3.1 (1.0)	3.1 (1.0)	3.1 (1.0)	6.8 (2.2)	6.8 (2.2)	0.87 (0.28)	0.87 (0.28)

Table 2: Bounds on c for $\Lambda = 1$ TeV, assuming one operator at a time, using the different signal regions defined in the text. The numbers without (within) parenthesis stand for the LHC13 (HL-LHC). The boldface indicates limits using actual data. These numbers can be obtained from the master equation (2.14) using the coefficients in Table 1 and the upper bound on the following number of signal events: $s_{\max}^{CR1} = 143$ (315) and $s_{\max}^{NEW} = 18$ (179), where again the number in brackets correspond to HL-LHC projections. The projected bounds on the coefficients get a factor of ~ 3 weaker for systematic uncertainties of 10%.

